A Dynamic User-Equilibrium Model with Travel Times Computed from Simulation

B.C. Khoo*, G.C. Lin†, J. Peraire‡, G. Perakis§

August 31, 2004

Abstract

The dynamic user-equilibrium problem has attracted much attention in recent years. Its application to traffic management and in particular, its connection to Intelligent Transportation Systems (ITS) makes the study of this problem particularly relevant. An important aspect involves the calculation of travel times. In this paper, we propose a new approach for calculating travel times through a path-based simulation model that predicts the evolution of traffic flows. The model we consider describes accurately the dynamics of the residence time of the vehicles in the network and does not require a-priori knowledge of the functional form of the link travel times in the network. Furthermore, we combine the travel time simulation model with a dynamic user-equilibrium model. To achieve this we consider a variational inequality formulation that incorporates the path travel times obtained from the simulation model. We introduce several variations of the Frank-Wolfe method for solving this variational inequality formulation. Finally, we present some numerical results that illustrate the performance of the proposed methods.

Keywords: Traffic flow, transportation networks, travel time, dynamic user-equilibrium

*Singapore-MIT Alliance and Department of Mechanical Engineering, National University of Singapore

†Singapore-MIT Alliance, National University of Singapore

‡Singapore-MIT Alliance and Department of Aeronautics, MIT

§Singapore-MIT Alliance and Sloan School of Management, MIT, corresponding author: georgiap@mit.edu

1 Introduction

User-equilibrium problems arise in a wide variety of application areas as diverse as urban transportation planning and management, routing messages in communication networks, mechanical systems, electric power systems and equilibrium problems in economics. Studying these problems is particularly important in the area of transportation due to traffic congestion which has become an increasingly acute phenomenon in urban and highway transportation systems.

In many settings the nature of traffic is inherently dynamic. One can just notice that time-of-the-day plays a major role in how transportation systems are utilized. For example, traffic flow patterns during rush hour are typically different from traffic flow patterns during other times of the day. Such phenomena cannot be easily modeled within the framework of static user-equilibrium models. On the other hand, dynamic user-equilibrium models are particularly useful in modeling these phenomena. Furthermore, the development of Intelligent Transportation Systems (ITS) has further strengthened the need for studying dynamic user-equilibrium problems.

There are two main categories of models in the literature for modeling the dynamic nature of traffic flow and travel times: macroscopic and microscopic models. Macroscopic models take an analytical approach. Lighthill and Whitham (1955) and independently Richards (1956) developed the first analytical model. This was extended by Payne (1971) and Whitham (1974). Furthermore, Papageorgiou (1998) and Heidemann (1999) and the references therein have studied macroscopic models further. This approach enables study of the analytical properties of the problem. However, some critics argue that it does not allow one to model as effectively some of the realism and underlying complexities of the problem in an accurate and detailed way. As a result, one can claim that it takes away some of the realism of the model. Nevertheless, from a theoretical perspective, it provides a deeper understanding of the properties of the model. Furthermore, this approach allows one to incorporate the underlying traffic flow dynamics within a variational inequality framework (see for example, Friesz *et al.* (1993), Ran and Boyce (1994), Ran *et al.* (1996), Perakis (2000)) and design solution algorithms.

The second category of models consists of microscopic (or called car-following) models. Such models have the ability to describe, at a level of detail, the network geometry, the traffic flow and its kinematics as well as the traffic control logic. Reuschell (1950) proposed the first car-following

model. Pipes (1953) and Herman *et al.* (1959) extended this model. Gerlough and Huber (1975), Bekey, Burnham and Seo (1977), Papageorgiou (1983), Papageorgiou, Blosseville and Haj-Salem (1989) and references therein provide an extensive analysis of these models.

Finally, there is a hybrid class of models (see for example, Daganzo (1994, 1995a, 1995b, 1995c), and Smith (1993)). Using this latter approach one handles the constraints describing the traffic flow dynamics separately from the equilibrium model describing the traffic assignment part of the problem. As a result, one solves the optimization model iteratively with updated travel times that arise from an independent simulation module (see Jayakrishnan *et al.* (1995)). As pointed out in Jayakrishnan *et al.* (1995), this class of simulation-based models can incorporate traffic control strategies easily and capture the traffic flow dynamics better through an independent traffic flow simulation model.

The literature in transportation takes on two approaches when modeling travel times. The first and more traditional approach assumes a predetermined functional form that describes the relationship between travel times and flow rates. This is typically determined through a statistical analysis. Practitioners in the transportation community have been using several functional forms to describe travel times. These include the BPR function (Bureau of Public Roads, 1964) which is used to estimate travel times at priority intersections, and is a polynomial function. Akcelik (1988) proposed a polynomial-type travel time function for links at signalized intersections. Meneguzzer *et al.* (1990) also proposed an exponential travel time function for all-way-stop intersections. Although these functions were developed in the context of static user-equilibrium problems, their dynamic analogues have also been used in a dynamic context. Nevertheless, considering a specific link travel time function in advance has some drawbacks. For instance, those functions often assume that the delay depends on the current traffic volume, the traffic inflow and outflow rate at a link. As a result, these travel time functions may not describe accurately peak period traffic dynamics especially since there are dramatic changes in traffic conditions in a short period of time. Travel times in a dynamic transportation network depend both on prevailing traffic conditions and future traffic conditions relative to the departure time. As a result, this approach can lead to controversial results (see Daganzo, (1994)). Recently, a second approach for modelling travel times considers travel time functions as an output rather than an input in the model (see Perakis

(2000) and Kachani and Perakis (2001a, b, c)). This approach determines the functional forms for travel times through an analytical method which solves the hydrodynamic model of Lighthill and Witham (1955). Kuwahara and Akamatsu (2001) also derived an analytical function of the instantaneous travel time in order to solve the dynamic user equilibrium. However, the travel time they derived does not represent the actual (or experienced) travel time, unless traffic conditions remain constant).

In this paper, we propose a framework which takes a hybrid approach and determines travel times which are also an output. This framework combines a simulation together with a variational inequality model. In particular, we consider a path-based simulation model which describes the traffic flow dynamics and as a result, allows us to determine path travel times. This simulation model consists of a system of equations which solution gives rise to path travel times for vehicles under a given traffic assignment. Furthermore, in order to study the overall dynamic user-equilibrium problem, we consider a variational inequality formulation using the travel times determined through the simulation module. Finally, we study two variations of the Frank-Wolfe method for solving the variational inequality formulation.

Our contributions in this paper are the following:

1. We propose a framework that integrates a variational inequality formulation for determining a dynamic user-equilibrium assignment together with a path-based simulation model for determining travel times in dynamic transportation networks.

2. We propose a path-based simulation model that consists of a set of equations describing the path flow dynamics. These equations are part of the overall framework rather than assuming their solution in advance. In particular, the simulation model we propose describes the vehicles' residence time through a system of partial differential equations. As a result, this simulation model determines actual path travel times.

3. We propose methods for solving the overall dynamic user-equilibrium problem and study their convergence properties numerically.

The remainder of the paper is organized as follows: In Section 2, we propose a dynamic route-choice user-equilibrium model through a variational inequality (VI) formulation in terms of path

flow departure rates. In Section 3, we introduce a path-based simulation model for determining path travel times. In Section 4, we discuss the integration of the variational inequality formulation and the simulation model as well as consider solution methods of the models. In Section 5, we present some numerical results to verify the validity of the overall framework.

2 A Dynamic User-Equilibrium Model – Notation and Problem Definition

The route choice user-equilibrium problem in the static case was first proposed by Wardrop (1952). A traffic user-equilibrium traffic flow has the property that once established, no traveler can decrease his/her travel cost by making a unilateral decision to change his/her route. This principle also extends to describe the dynamic user-equilibrium problem as follows. Friesz *et al.* (1993) were among the first to formulate the dynamic user-equilibrium problem and study existence of solution.

Dynamic User-Equilibrium (DUE): *For every time instant, the experienced path travel times on used routes connecting an origin-destination (O-D) pair are equal and minimal.*

Consider a transportation network represented via a directed network $G = (\mathcal{N}, \mathcal{E})$, where $\mathcal{N}$ is the set of nodes and $\mathcal{E}$ is the set of directed links. Let $k = (o, d)$ be an O-D pair with origin node o and destination node d, where $o, d \in \mathcal{N}$. Set O denotes the set of all O-D pairs, and P_k the set of available routes between O-D pair k. $D_k(t)$ denotes the traffic demand rate for O-D pair k at time t, and $D_p(t)$ the demand for path p. $f_{k,p}(t)$ denotes the path flow departure rate corresponding to path p at time t (in this case, path $p \in P_k$). Vector $\mathbf{f}(t)$ denotes the vector of path flow departure rates $f_{k,p}(t)$, for all paths at time t, and $\mathbf{f}$ represents path flow departure rates over the entire time horizon. The time horizon is the interval $[0, T]$. $h_{k,p}(t)$ denotes the (experienced) path travel time at time t for path p. The value of $h_{k,p}(t)$ is affected by the initial traffic conditions and traffic assignment flow $\mathbf{f}$ over time horizon $[0, T]$. Since different path flow assignments have different effects on path travel times, we write $h_{k,p}(t)$ as a function of $\mathbf{f}$ and time t, that is, $h_{k,p}(\mathbf{f}, t)$. Furthermore, we denote the feasible region of path flow rates $\mathbf{f}$ as $\mathcal{K}$.

Any flow rate vector $\mathbf{f} \in \mathcal{K}$ satisfies the following feasibility conditions:

$$\begin{aligned} \textstyle\sum_{p \in P_k} f_{k,p}(t) = D_k(t) \quad & \forall k \in O, t \in [0,T]; \\ f_{k,p}(t) \geq 0 \qquad\quad & \forall k \in O, p \in P_k, t \in [0,T]. \end{aligned} \tag{1}$$

As a result, the dynamic user-equilibrium problem can be written as follows:

DUE formulation: For $t \in [0,T]$, given a traffic demand rate $D_k(t)$, find $\mathbf{f} \in \mathcal{K}$ satisfying

$$f_{k,p}(t)[h_{k,p}(\mathbf{f},t) - m_k(t)] = 0 \quad \forall k \in O, p \in P_k, t \in [0,T]; \tag{2}$$

$$m_k(t) = \min_{p \in P_k} \{h_{k,p}(\mathbf{f},t)\} \qquad \forall k \in O, t \in [0,T]. \tag{3}$$

These conditions imply that if $f_{k,p}(t) > 0$, $h_{k,p}(\mathbf{f},t) = m_k(t)$, and if path p is used, the travel time to traverse it is equal to the minimal path travel time for O-D pair k at time t. Furthermore, if $h_{k,p}(\mathbf{f},t) - m_k(t) > 0$ then $f_{k,p}(t) = 0$. This implies that if at time t, a path travel time is bigger than the minimal path travel time, then there is no traffic on this path at time t. Notice that these constraints are consistent with the definition of the dynamic user-equilibrium problem.

The path travel time $h_{k,p}(\mathbf{f},t)$ is no longer a function of a static link flow rate but depends on dynamic flow rates over the entire time horizon. Furthermore, notice that no assumption is made on the symmetry of the Jacobian matrix of $h_{k,p}(\mathbf{f},t)$. This lack of symmetry adds a further degree of difficulty in the solution of the dynamic traffic user-equilibrium problem, since there is no underlying optimization problem.

Nevertheless, by considering travel times that arise from an independent simulation model, we are able to eliminate some of the difficulties caused by traffic flow relationships. Furthermore, we incorporate these travel times in the following equivalent variational inequality formulation:

VI formulation of DUE: Find $\mathbf{f}^* \in \mathcal{K}$ satisfying

$$\int_0^T \sum_{k \in O} \sum_{p \in P_k} h_{k,p}(\mathbf{f}^*,t)[f_{k,p}(t) - f^*_{k,p}(t)]dt \geq 0, \qquad \text{for any } \mathbf{f} \in \mathcal{K}. \tag{4}$$

We denote by $\mathbf{f}^*$, the flow of a traffic assignment satisfying the DUE conditions. The proof of the equivalence between this VI formulation and the DUE conditions (2) can be found in Ran and Boyce (1994).

In this paper, the path travel time $h_{k,p}(\mathbf{f},t)$, for any time instant t, depends on the traffic assignment $\mathbf{f}$ over the entire time horizon. This is different from other approaches which assume

that the travel time is determined only by the prevailing traffic conditions at that time. In reality, path travel times depend not only on the prevailing traffic conditions but also on future traffic conditions, especially on traffic inputs on other parts of the network.

In what follows, we consider a discrete version of the problem. To achieve this we discretize the time horizon in the VI formulation at Equation (4). Denote $\hat{h}^n_{k,p}$ as the discrete path travel time on path p at the nth time interval. Similarly, $\hat{f}^n_{k,p}$ is the discrete path flow departure rate on path p, at the nth time interval. Vector $\hat{\mathbf{f}}$ denotes the vector of discrete traffic flows on the entire time horizon. There is a total of N time intervals. The discretized feasible region $\hat{\mathcal{K}}$ satisfies the following feasibility conditions:

$$\sum_{p \in P_k} \hat{f}^n_{k,p} = \hat{D}^n_k \qquad \forall k \in O; n = 1 \ldots N \tag{5}$$

$$\hat{f}^n_{k,p} \geq 0 \quad \forall k \in O, p \in P_k; n = 1 \ldots N \tag{6}$$

We are now able to formulate the following discretized variational inequality problem.

Discretized VI formulation: Find $\hat{\mathbf{f}}^* \in \hat{\mathcal{K}}$ satisfying

$$\sum_{n=1}^{N} \sum_{k \in O} \sum_{p \in P_k} \hat{h}^{n^*}_{k,p} (\hat{f}^n_{k,p} - \hat{f}^{n^*}_{k,p}) \geq 0, \quad \text{for any } \hat{\mathbf{f}} \in \hat{\mathcal{K}}. \tag{7}$$

This formulation will be particularly useful in proposing methods for solving the dynamic user-equilibrium problem.

3 Evaluation of Path Travel Times via Simulation

In this section, we discuss a path-based continuum flow model describing traffic and its numerical solution. Based on this model an approach for extracting path travel times is presented.

3.1 A path-based simulation model for traffic flows

3.1.1 Model for a single link

Let us consider a link joining two nodes of a transportation network. Following the hydrodynamic theory of traffic flows of Lighthill and Whitham (1955), and Richards (1956), we define the car density $\rho(x,t)$ as the number of cars per unit length of road. This car density is a function

of the position x, measured along the link, and the time t. Let $u(x,t)$ denote the average car velocity, also at position x and time t. Then, the flow rate, or flux $F(x,t)$, will be given by $F(x,t) = \rho(x,t)u(x,t)$ and the differential equation expressing car conservation is written as

$$\frac{\partial \rho}{\partial t} + \frac{\partial F}{\partial x} = 0 \ . \tag{8}$$

This equation can be integrated in time for the unknown ρ, provided the velocity is either given or expressed as a function of the car density. In practice, it is customary to express the velocity as a function of the density. This functional dependence can be linear or nonlinear. Although linear velocity-density relationships have some well-known deficiencies (see TRB, 1997), they are sufficient for our purpose of introducing our path-based simulation model. In this paper we use the Greenshields linear velocity-density relationship, which is given by,

$$u(x,t) = u^{max}(1 - \frac{\rho(x,t)}{\rho^{max}}) \ . \tag{9}$$

In this equation the parameters ρ^{max} and $u^{\max}$ are the maximum density and velocity, respectively. This relation shows a linear variation of the velocity with the density between the maximum velocity, at zero density, and a zero velocity, at maximum density. When expression (9) is inserted into (8), the flux becomes a function of the car density and we obtain a non-linear conservation law. It is well known that the solution of this equation may contain discontinuities, or shocks, even if the initial and boundary conditions are continuous. Despite its simplicity this model is able to capture many of the qualitative features observed in real traffic. Although analytical solutions for this equation can be found for simple initial and boundary data, our approach will be to solve this equation numerically so that general situations can be handled. In addition, the numerical solution can be easily extended to more complex non-linear velocity-density relations.

The link under consideration is discretized into a number of equal intervals of length Δx. The time interval $[0,T]$ is also discretized into N intervals of size Δt. A standard explicit finite volume algorithm (LeVeque (1990)) for equation (8) reads,

$$\rho^{j,n+1} = \rho^{j,n} - \frac{\Delta t}{\Delta x}(F^{j+1/2,n} - F^{j-1/2,n}) \ . \tag{10}$$

Here, $\rho^{j,n}$ is an approximation to $\rho(x^j, t^n)$, and the $F^{j+1/2,n}$ is an approximation to $F(\rho(x^{j+1/2}, t^n))$, where $x^j = j\Delta x$ and $t^n = n\Delta t$. The choice of the approximate flux function completely determines the numerical scheme. In this paper we have chosen a simple first order Godunov method.

More sophisticated and accurate schemes could also be implemented but we have not found it to be necessary at this point. In Godunov's method, the flux function, $F^{j+1/2,n}$ is a function of $\rho^{j,n}$ and $\rho^{j+1,n}$ only, and is given by,

$$F^{j+1/2,n} = \min_{\rho\in[\rho^{j,n},\rho^{j+1,n}]} F(\rho), \qquad \text{if} \quad \rho^{j,n} < \rho^{j+1,n} \tag{11}$$

$$F^{j+1/2,n} = \max_{\rho\in[\rho^{j,n},\rho^{j+1,n}]} F(\rho), \qquad \text{if} \quad \rho^{j,n} \geq \rho^{j+1,n} \quad . \tag{12}$$

The details can be found in LeVeque (1990). It is worth reinforcing the fact that this flux can always be written as $F^{j+1/2,n} = F(\rho^*)$, where ρ^*, is a value of the car density in the interval $[\rho^{j,n}, \rho^{j+1,n}]$. It is easy to verify that depending on the values of $\rho^{j+1,n}$ and $\rho^{j,n}$, ρ^* can only be $\rho^{j,n}$, $\rho^{j,n+1}$ or $\rho^{max}/2$. The scheme (10) with flux functions given by (11) or (12) is stable provided $\Delta t \leq u^{max}/\Delta x$.

3.1.2 Link shared by multiple paths

In general, a given link will be used by more than one path and we will be interested in tracking the densities of the cars corresponding to the different paths. Let $\mathcal{P}$ be the set of paths that share a given link. If $\rho_p(x,t)$ denotes the density of cars on that link following path p, then clearly,

$$\rho(x,t) = \sum_{p\in\mathcal{P}} \rho_p(x,t) \ . \tag{13}$$

In order to be able to time advance each of the densities, $\rho_p(x,t)$, individually, we write a conservation equation for each $p \in \mathcal{P}$,

$$\frac{\partial \rho_p}{\partial t} + \frac{\partial F_p}{\partial x} = 0 \ . \tag{14}$$

Given condition (13), it is clear that we want to choose the fluxes F_p , so that,

$$F(\rho) = \sum_{p\in P} F_p \ . \tag{15}$$

This is easily accomplished if we realize that, at a given location, the velocity for all the cars must be the same regardless of the path they are following. In addition, this velocity will be a function of the total car density. Thus, we write,

$$F_p = \rho_p u(\rho) \ . \tag{16}$$

In order to solve numerically the system of equations (14) we write for each $p \in \mathcal{P}$, a discrete equation of the form,

$$\rho_p^{j,n+1} = \rho_p^{j,n} - \frac{\Delta t}{\Delta x}(F_p^{j+1/2,n} - F_p^{j-1/2,n}) \ . \tag{17}$$

The choice of the numerical flux approximations is now less obvious because here, we are dealing with a system of equations rather than a scalar equation. Our design criterion is that the discrete evolution equations should be such that when added over all the paths sharing the same link, the resulting equation should be consistent with equation (10) for the total density. In order to accomplish that, we proceed as follows. With the value of the total car density at $\rho^{j,n}$ and $\rho^{j+1,n}$, use expressions (11) and (12) to determine ρ^*. That is,

$$\rho^* = \arg \min_{\rho \in [\rho^{j,n}, \rho^{j+1,n}]} F(\rho), \qquad \text{if} \quad \rho^{j,n} < \rho^{j+1,n} \tag{18}$$

$$\rho^* = \arg \max_{\rho \in [\rho^{j,n}, \rho^{j+1,n}]} F(\rho), \qquad \text{if} \quad \rho^{j,n} \geq \rho^{j+1,n} \quad . \tag{19}$$

Evaluate $\eta = \frac{\rho^{j+1,n} - \rho^*}{\rho^{j+1,n} - \rho^{j,n}}$, such that

$$\rho^* = \eta \rho^{j,n} + (1-\eta)\rho^{j+1,n} \ , \tag{20}$$

and finally compute $F_p^{j+1/2,n}$, for each $p \in \mathcal{P}$, as

$$F_p^{j+1/2,n} = (\eta \rho_p^{j,n} + (1-\eta)\rho_p^{j+1,n}) u(\rho^*) = (\eta \rho_p^{j,n} + (1-\eta)\rho_p^{j+1,n}) u^{max}(1 - \frac{\rho}{\rho^{max}}) \ . \tag{21}$$

3.1.3 Traffic lights

The modeling of a traffic light controlled intersection is straightforward. At the location of the traffic light, we set the flux equal to zero when the light is red. Although realistic intersections occupy some length of space, we treat intersections as being concentrated at a point.

3.1.4 Variable link parameters

In the two previous sections, we have implicitly assumed that the parameters that determine the road capacity ρ^{max}, and maximum velocity u^{max}, are constant along the link. In some cases, it will be necessary to be able to handle situations in which these properties change. In particular, this feature will be exploited to model link intersection without traffic lights. Our objective here

is to determine how to extend the flux functions (11) and (12), to the situation in which the link parameters before the interface, i.e. point j, are $(\rho_-^{max}, u_-^{max})$ whereas the link parameters after the interface , i.e. point $j+1$, are $(\rho_+^{max}, u_+^{max})$. In this case, the decision on whether to use the value of the flux determined by the state before or after the interface needs to be based on the local slope of the characteristic curves (see for instance LeVeque (1990)). This is given by the value of $a(\rho) = dF(\rho)/d\rho$. Using Greenshields linear velocity-density relationship, it follows that, $a_- = u_-^{max}(1 - 2\rho_-/\rho_-^{max})$ and $a_+ = u_+^{max}(1 - 2\rho_+/\rho_+^{max})$. The procedure for evaluating the numerical flux $F^n \equiv F^{j+1/2,n}$ at the interface becomes

$$F^n = \begin{cases} F_-^n & \text{if } a_-^n \geq 0,\ a_+^n \geq 0 \\ F_+^n & \text{if } a_-^n \leq 0,\ a_+^n \leq 0 \\ \min(F_-^n, F_+^n) & \text{if } a_-^n \geq 0 \geq a_+^n \\ \min(\frac{\rho_- u_-^{max}}{2}, \frac{\rho_+ u_+^{max}}{2}) & \text{if } a_-^n \leq 0 \leq a_+^n \end{cases} . \tag{22}$$

It is straightforward to verify that when the link parameters are constant the above expressions are equivalent to (11) and (12).

3.1.5 Link boundary conditions

Boundary conditions on each link are specified by determining the fluxes at the beginning and at the end of each link. When several paths share the same link, the fluxes for each of the paths need to be specified. It is clear that at the network nodes, where the links intersect, we must have car conservation. That is, the sum of all the fluxes into the node must equal the sum of all the fluxes out of the node. In addition, this must be true for each path separately. There are several ways in which link intersections can be modeled. One option, as discussed above, is with traffic lights which cycle between green and red at prescribed intervals. Alternatively, we can have uncontrolled intersections. Here also, cars coming from one link, or following a specific path, can be given priority over other cars. If this is the case, this should be reflected in the way intersections are modeled. In our model, we have followed a simple approach which assumes that no car is given a preferential treatment. If a link is shared by several paths, we assume that the road capacity ρ^{max}, is shared by each of the paths in an amount which is proportional to the corresponding path car density ρ_p, at that point. That is, the road capacity allocated to path

p, is given by $\rho_p^{max} = \rho_p \rho^{max}/\rho$. This is done for both, the inflow and the outflow links. For each path, say exiting link i, and going into link i', we compute the flux F_p using expressions (22) and the corresponding parameters for links i and i'. That is, for link i we set $u_-^{max} = u_i^{max}$, and $\rho_-^{max} = (\rho_p)_i(\rho^{max})_i/(\rho)_i$, whereas for link i', we set $u_+^{max} = u_{i'}^{max}$, and $\rho_+^{max} = (\rho_p)_{i'}(\rho^{max})_{i'}/(\rho)_{i'}$. The corresponding flux for each link is obtained by adding up the fluxes of all the paths sharing that link.

At the departure points, we calculate the maximum capacity flux by setting ρ_- in (22), equal to $\rho_-^{max} = \rho_+^{max}$, and $u_-^{max} = u_+^{max}$. If the demand flux is less than the maximum capacity flux we set the flux equal to the demand flux. If the demand flux is higher than the maximum flux then, the demand can not be satisfied, and in this case we set the flux equal to the computed maximum flux.

At the outflow destination points we calculate flux by setting $\rho_+ = 0$, and $\rho_+^{max} = \rho_-^{max}$, and $u_+^{max} = u_-^{max}$, and using expressions (22).

3.2 Extracting travel times from the simulation results

In the literature, it is common to use the term travel time to refer to two different concepts. One of them is the time experienced by the traveler and takes into account the changing travel conditions which may occur after its departure. Sometimes this travel time is called the *actual path travel time*. Alternatively, the travel time may denote the travel time that would be experience by the traveler if the traffic conditions at the time of departure were to remain unchanged until the traveler reaches the destination point. This later travel time may also be referred to as the *instantaneous path travel time*. In our simulation model we employ the actual path travel time.

Our approach to computing travel times consists of solving simultaneously for the car densities, $\rho(x,t)$, as shown in the previous section, and for the residence time $\tau(x,t)$. The residence time is defined at each point in space and time, as the time the traveler has been on the road since the time of departure. The differential equation satisfied by $\tau(x,t)$ is

$$\frac{D\tau}{Dt} = 1 \ , \tag{23}$$

which simply states that the clock of the traveler will increase by one unit every unit of time. Here, we have used a material derivative to indicate that τ "moves" with the cars. The corresponding

partial differential equation is therefore

$$\frac{\partial \tau}{\partial t} + u(x,t)\frac{\partial \tau}{\partial x} = 1 \ . \tag{24}$$

In order to solve numerically the hyperbolic PDE for the travel time τ, we use a simple upwind scheme here. The discretized equation is written as,

$$\tau^{j,n+1} = \tau^{j,n} - \frac{\Delta t \ u^{j,n}}{\Delta x}(\tau^{j,n} - \tau^{j-1,n}) + \Delta t \ . \tag{25}$$

This numerical scheme has the attractive property that will produce solutions for the travel time which are monotonically increasing in space, as expected. This can be easily seen if we write the difference between equation (25) evaluated at two successive spatial nodes,

$$\begin{aligned} \tau^{j,n+1} - \tau^{j-1,n+1} &= \tau^{j,n} - \tau^{j-1,n} - C^{j,n}(\tau^{j,n} - \tau^{j-1,n}) + C^{j-1,n}(\tau^{j-1,n} - \tau^{j-2,n}) \\ &= (1 - C^{j,n})(\tau^{j,n} - \tau^{j-1,n}) + C^{j-1,n}(\tau^{j-1,n} - \tau^{j-2,n}) \ . \end{aligned}$$

where $C^{j,n} = \Delta t u^{j,n}/\Delta x$ is the Courant number. Assuming that the travel time at time level n is monotonically increasing, and that $0 \leq C^{j,n} \leq 1$, as required for stability, for any j, then $\tau^{j,n+1} - \tau^{j-1,n+1} \geq 0$ for all j.

In our simulation we may have several paths sharing the same link. In this case we write for each path $p \in \mathcal{P}$, an equation of the form

$$\frac{\partial \tau_p}{\partial t} + u(x,t)\frac{\partial \tau_p}{\partial x} = 1. \tag{26}$$

which is solved with the scheme (25) for each p.

Boundary conditions for this equation are very simple. At the beginning of each link the values of τ_p is the same as that at the end of the previous link, and at the path origin τ_p is equal to zero. The initial conditions are normally set to the time it will take for a car to arrive at position x starting at the origin and traveling, say, at the maximum speed. It turns out that the initial condition has no effect on the solution after the time in which the first car in the path reaches its destination.

If L_p is the length of the path p, then the travel time will be simply $\tau(L_p, t)$. In our optimization model however, we will be interested in knowing the travel time as a function of the departure time

rather than the actual time. If t_d denotes the departure time, at time t the following relationship will be satisfied

$$t = t_d + \tau_p(x, t) \tag{27}$$

So we know that for vehicles on path p, if they arrive at the destination at time t, their travel time is represented by $\tau_p(L_p, t)$, these vehicles' departure time is computed by $t - \tau_p(L_p, t)$.

4 Solving the DUE Model using Travel Times from a Simulation Module

In this section we propose a method for solving the combined dynamic travel time and dynamic user-equilibrium model (DUE). This approach integrates the simulation module discussed in the previous section with the variational inequality formulation (4).

The key idea is in combining iteratively the evaluation of path travel times through the simulation module together with the solution of the discretized variational inequality problem (7) that determines a dynamic user-equilibrium flow pattern. As a result, the traffic flow on each path serves as input to the simulation module while the path travel times corresponding to this traffic flow are the output. Furthermore, at each iteration in the variational inequality component of the method, the path travel times that arise from the simulation module serve as input while the output is the new traffic assignment (that is, the path flow departure rates). This in turn becomes the new input to the simulation module.

We solve the variational inequality formulation (4) through a dynamic version of the Frank-Wolfe (FW) method. This method is known to converge to a user-equilibrium solution for symmetric static traffic assignment problems (see Frank and Wolfe (1956)). Furthermore, under some additional assumptions on the degree of asymmetry of the problem, the Frank-Wolfe method also converges for asymmetric problems (see Magnanti and Perakis (1998)).

We consider several variations of the Frank-Wolfe method for solving the dynamic user-equilibrium problem. We illustrate the convergence of these methods through a numerical study. Nevertheless, it may be noted that their theoretical convergence remains an open issue for asymmetric dynamic traffic equilibrium problems.

First we note that vector $\hat{\mathbf{f}}^i$ denotes the solution of the dynamic user-equilibrium problem at the ith iteration. The procedure of a Frank-Wolfe method for solving the dynamic user-equilibrium problem is as follows:

Step 0: Find an initial feasible path flow departure rate $\hat{\mathbf{f}}^0$. (Note that it is easy to find such a vector through an *all-or-nothing* assignment at every O-D pair or if over-saturation flow appears by splitting the flow into several routes). Set iteration count i as $i := 1$.

Step 1: At iteration i, using $\hat{\mathbf{f}}^{i-1}$ as input, run the simulation module until all the vehicles arrive at their destinations. The simulation module outputs a path travel time $\hat{\mathbf{h}}$, the vector of path travel time $\hat{h}^n_{k,p}$.

Step 2: Using the path travel time from **Step 1**, solve the following linear programming problem.

$$\begin{aligned} \min_{\hat{\mathbf{f}}} \quad & \textstyle\sum_n \sum_k \sum_p \hat{h}^n_{k,p}\ \hat{f}^n_{k,p} \\ s.t. \quad & \textstyle\sum_p \hat{f}^n_{k,p} = \hat{D}^n_k, \qquad \forall\ k \in O; n = 1 \ldots N \\ & \hat{f}^n_{k,p} \geq 0, \qquad \forall\ k \in O, p \in P_k; n = 1 \ldots N. \end{aligned}$$

We denote an optimal solution for this problem as $\hat{\mathbf{f}}^*$.

Step 3: Perform a line search in the segment $[\hat{\mathbf{f}}^{i-1}, \hat{\mathbf{f}}^*]$ through the solution of the following one-dimensional variational inequality problem:

Find $\alpha^* \in [0, 1]$ satisfying

$$\sum_n \sum_k \sum_p \hat{h}^n_{k,p}(\hat{\mathbf{f}}(\alpha^*))(\hat{f}^n_{k,p}(\alpha) - \hat{f}^n_{k,p}(\alpha^*)) \geq 0, \forall \alpha \in [0, 1],$$

where $\hat{\mathbf{f}}(\alpha) = \alpha\hat{\mathbf{f}}^{i-1} + (1 - \alpha)\hat{\mathbf{f}}^*$. Set $\hat{\mathbf{f}}^i := \hat{\mathbf{f}}(\alpha^*)$.

Step 4: Convergence verification. We define $C = \sum_k c_k$, where c_k is

$$c_k = \sum_n \sum_p (\hat{h}^n_{k,p} - \hat{m}^n_k)\hat{f}^n_{k,p}.$$

If $C \leq \epsilon$, stop. Otherwise, set $i := i + 1$, and repeat from **Step 1**.

Some remarks:

1. In the line search procedure in **Step 3**, there is no need of the explicit form of the travel time function $\hat{h}^n_{k,p}(\hat{\mathbf{f}})$. We use an iterative procedure to perform the line search without a-priori knowledge of the functional form by using the results of the simulation module.

2. In our numerical analysis we consider further two variations of the Frank-Wolfe method. These methods attempt to resolve some practical issues on the speed of convergence of the Frank-Wolfe method. The two variations considered are: (i) an Affine-Scaling version of the Frank-Wolfe method (see Perakis and Zaretsky (2002)), this method restricts at each step the feasible region of the optimization problem we solve in order to compute the descent direction at **Step 2**. In particular, we consider in the optimization problem an ellipsoid that depends on the current iterate and which always contained in the original feasible region. The purpose of this modification is to reduce the zigzagging behavior of the method. Here is the additional constraint imposed:

$$||(\mathbf{F}^{i-1})^{-1}\mathbf{d}|| \leq r$$

where $\mathbf{d} = \hat{\mathbf{f}} - \hat{\mathbf{f}}^{i-1}$, $\mathbf{F}^{i-1}$ is the diagonal matrix of vector $\hat{\mathbf{f}}^{i-1}$, r is a constant. (ii) a hybrid method which combines the Affine-Scaling together with the Frank-Wolfe method. This hybrid method takes advantage of the insights gained from the Frank-Wolfe method and the Affine-Scaling version of the method by using the Frank-Wolfe method for the first several iterations and subsequently in the later iterations (since close to the solution the Frank-Wolfe method tends to be slow) switching to the Affine-Scaling method.

5 Numerical Results

In this section, we present some numerical results for the path travel time calculation by simulation and the framework which combines the simulation module with the variational inequality formulation.

5.1 Computational Results for the Simulation Model

We test the simulation model with two network examples. In the first example, the network has traffic-light controls while in the second example the network has no traffic-light controls. For

both networks, we calculate the path travel times.

Figure 1 illustrates network 1. In this example, there is one intersection controlled by a traffic light at node D. The traffic light is controlled by setting at every period equal green time for the three connecting in-links. The length of links 1, 2, and 3 is 1 *unit*, respectively. The length of link 4 is 3 *units*. There are three paths in network 1 namely, (links 1 and 4), (links 2 and 4) and (links 3 and 4). The traffic light at intersection D is controlled in the following way: every link has a two-unit green time. The inflow in paths 1, 2 and 3 is 0.2 *units* respectively. The maximum velocity is set to be 1 *unit*, while the maximum density is also set to be 1 *unit*.

Figure 2 shows the calculated path travel times corresponding to different departure times. The results in these figures indicate that the path travel times are discontinuous. This is consistent with what happens in reality in networks with traffic light-controlled intersections. Moreover, the gap between the maximum path travel time and the minimum path travel time is about the same as the red light time. This time is four units in this example.

In the second example, we consider a more complex network. Network 2 is shown in Figure 3.It is taken from Xu *et al.* (1999), and so are the relevant parameters. Table 1 shows all the O-D pairs with nonzero demands and all the paths in the network. The paths are grouped according to O-D pairs.

In network 2, we assume that all the links have the same maximum density and maximum velocity. Nevertheless, we allow different values for the two parameters. The maximum density ρ^{max} is 200 $vehicles/mile$ while the maximum velocity u^{max} is 40 $miles/hour$. Suppose the simulation time period is from 0 to T. The traffic demand for path k is defined through the following function:

$$D_k(t) = \begin{cases} \theta_k(\frac{4f^{max}}{T}t - \frac{4f^{max}}{T^2}t^2) & 0 \leq t \leq T \\ 0 & t > T, \end{cases} \tag{28}$$

where $k = 1, \ldots, 14$. Notice that f^{max} denotes the maximum flow rate, calculated as $f^{max} = 0.25\ \rho^{max}\ u^{max}$. The coefficient θ_k and the length of each link are shown in Table 2.

Figure 4 and 5 shows the path travel times calculated. The calculated path travel times demonstrate dynamic features and are consistent with the intuition that the maximum travel

Table 1: O-D pairs and paths

O-D pair	Path
(a,i)	1:(1,2,6,10)
	2:(1,5,7,10)
	3:(1,5,9,12)
	4:(3,4,7,10)
	5:(3,4,9,12)
	6:(3,8,11,12)
(a,e)	7:(1,5)
	8:(3,4)
(e,i)	9:(7,10)
	10:(9,12)
(a,c)	11:(3,8)
(c,i)	12:(11,12)
(a,g)	13:(1,2)
(g,i)	14:(6,10)

Table 2: Parameters for the paths in Network 2

path	θ_k	link j	length (miles)
1	0.10	1	2.0
2	0.15	2	2.0
3	0.18	3	1.5
4	0.20	4	1.8
5	0.10	5	1.5
6	0.12	6	2.1
7	0.20	7	1.7
8	0.10	8	1.8
9	0.15	9	2.0
10	0.15	10	2.3
11	0.12	11	2.2
12	0.10	12	2.5
13	0.10		
14	0.35		

time occurs when the path departure flow rates are maximum. In this case, the maximum path departure flow rates occur at time $t = \frac{T}{2}$. The plot of path travel times with different departure times is also given in Xu *et al.* (1999). However, in that paper, link cost functions are an input in the calculation of path travel times. As a result, only a qualitative comparison with the results in Xu *et al.* (1999) is meaningful.

We also compare our results with those obtained from the Cell Transmission Model (see Daganzo 1994, 1995a). The network used is a single link network. The length of the link is 4 $miles$, with $u_{max} = 40$ $miles/hour$, $\rho_{max} = 200$ $vehicles/mile$. The function describing the demand rate is given by the expression

$$d(t) = 1600 - 6400 \times (t - 0.5)^2, \tag{29}$$

where the simulation time t lasts from 0 to 1 hour. The plot of cumulative link departure/arrival vehicle number is shown in Figure 6. The dotted line represents the results from our model while the solid line illustrates the results from the Cell Transmission Model (CT model). The latter results are produced using a software program developed by Daganzo called NETCELL. The link travel time can be derived from the plots by calculating the time gap between the corresponding two points on any arrival/departure pair of curves with the same cumulative number. The results are comparable for the two models. This further demonstrates the effectiveness of the path-based simulation model introduced in this paper.

5.2 Numerical results for the variational inequality formulation

In this subsection, we show some numerical results from the solution of the variational inequality formulation. As discussed in Section 4, we consider three additional methods that are variations of the Frank-Wolfe method. This allows us to compare the convergence of these methods and use their results to establish the relative merit of each of these methods.

5.2.1 Equilibrium Solutions

The same transportation network shown in Figure 3 is used here. The traffic demands for O-D pair is decided by the following formula:

$$D_{r,s}(t) = \begin{cases} \theta_{r,s}(\frac{32}{T}t - \frac{32}{T^2}t^2) & 0 \leq t \leq T \\ 0 & t > T, \end{cases} \tag{30}$$

where $\theta_{r,s}$ is an O-D pair (r,s) relevant parameter. In this experiment, we use each O-D pair's first path's θ_k parameter as the value of $\theta_{r,s}$, using the same values from Table 2. From Table 2, we know that the $\theta_{a,i} = 0.1$. For this calculation, $T = 2$, the step size in time $\Delta t = 0.016$, step size in space $\Delta x = 0.02$, and $u_{max} = 0.8$, $\rho_{max} = 50$. In this experiment, we only present the results for one O-D pair: (a,i), by ignoring other O-D pairs' results. We decide whether the traffic assignments are equilibrium satisfying by checking each O-D pair independently. So it is sufficient for us to examine the solution property by using only one O-D pair. The Frank-Wolfe method is used for this calculation. Figure 7 illustrates the demand curve for O-D pair (a, i). Notice there are six different paths connecting this O-D pair. Figure 8 shows the initial traffic assignment for O-D pair (a, i). Figure 9 is the plot of path travel times under the traffic assignment pattern in Figure 8. The traffic assignment pattern in Figure 8 is not equilibrium satisfying since only Path 2 has traffic, but there are other paths (for example, Path 4) with smaller path travel time than Path 2. Figure 10 shows the path travel times corresponding to the six paths of the O-D pair (a,i) after twenty Frank-Wolfe iterations. Figure 11 shows the traffic assignment on the six paths given the O-D pair demand shown in Figure 7. This is a near equilibrium-satisfying solution since from Figure 10, Path 2 and 4 have smaller path travel times when compared with the other paths. This leads to the conclusion that no path other than Path 2 and 4 should be used. Figure 11 verifies this observation, since only Path 2 and 4 have nonzero traffic flow. Furthermore, for the departure time period from 0.8 to 1.4, Path 2 and 4 have equal and minimal path travel times. Figure 11 shows that in this time period, only Path 2 and 4 have nonzero traffic flows. For other periods, Path 4 has the smallest path travel time and all the flow is assigned to Path 4. The solution is consistent with the definition of the dynamic user-equilibrium (DUE) problem discussed in Section 2. We have also tested this behavior for different initial traffic assignments (results not shown). All the examples considered produce near user-equilibrium solutions after

20 Frank-Wolfe iterations. This suggests that the Frank-Wolfe method for solving the dynamic user-equilibrium problem that uses travel times from simulation produces reasonable solutions only after a few iterations.

5.2.2 Comparison of the convergence between the three different methods

In this subsection we compare the performance of the three methods considered. Figure 12 shows the convergence plot of these three methods. We consider 20 iterations of these methods and examine the convergence behavior of each. The error in the figure is the convergence factor C. That is:

$$Error = \sum_n \sum_k \sum_p (\hat{h}^n_{k,p} - \hat{m}^n_k)\hat{f}^n_{k,p}.$$

Notice that as we approach a user-equilibrium solution the $Error$ tends towards zero. The results show that the Frank-Wolfe (FW) method converges fast in the first several iterations. Nevertheless, the method demonstrates some zigzagging when near an equilibrium solution. The Affine-Scaling version of the FW method always converges in the descent direction. Nevertheless, the convergence speed is very slow. Figure 13 further illustrates the convergence speed of the Affine-Scaling version of the FW method. The hybrid method that combines the Frank-Wolfe with the Affine-Scaling method performs better than the Frank-Wolfe method in the last several iterations.

6 Conclusions

In this paper, we studied the dynamic user-equilibrium problem by proposing a framework which integrates a simulation module for determining travel times together with a variational inequality formulation for determining the user-equilibrium flow assignment. In particular,

(i) We proposed a path-based simulation model for determining travel times in dynamic transportation networks. One of the characteristics of the model is the conservation of path flows. This is different from other results in the literature which only address the dynamics of link flows. The simulation model can be a powerful tool for providing path related information such as path travel times and path flow rates. Furthermore, the simulation model in this paper incorporates

path-based traffic controls. This is lacking in most simulation models in the literature.

(ii) We proposed a model for describing the dynamics of the residence time of the vehicles traveling in the network. The model solves a hyperbolic partial differential equation (PDE). Using the path-based simulation model for traffic flows, one is able to describe the link and path travel time in an accurate way. As a result, we believe that this approach may be a better choice for determining travel times than conventional methods.

(iii) To determine a dynamic user-equilibrium solution, we also incorporated a variational inequality formulation in the overall framework. This formulation determines a dynamic route-choice user-equilibrium solution, in which the path travel time information is obtained from the path-based simulation model.

(iv) We proposed three methods for solving this variational inequality formulation. These methods are variations of the Frank-Wolfe method.

(v) Furthermore, we tested the integrated simulation and variational inequality framework and the methods proposed for solving it through a numerical study. The results indicate that these methods indeed compute a dynamic route-choice user-equilibrium solution.

We believe that the overall framework proposed and studied in this paper could have an impact in several application areas and in particular, to transportation as it could play a significant role in the development of intelligent route guidance systems.

References

[1] Akcelik, R. (1988). Capacity of a Shared Lane. Australian Road Research Board Proceedings 14(2), 228-241.

[2] Bekey, A., Burnham, G., and Seo, J. (1977). Control theoretic models of human drivers in car following. Hum. Factors, (19),399–413.

[3] Bureau of Public Roads (1964). Traffic Assignment Manual. US Department of Commerce, Washington, DC.

[4] Daganzo, C. F. (1994). The Cell Transmission Model: a Dynamic Representation of Highway Traffic Consistent with the Hydrodynamic Theory. Transpn. Res. B, Vol. 28B, No. 4, pp. 269-287.

[5] Daganzo, C. F. (1995a). The Cell Transmission Model, Part II: Network Traffic. Transpn. Res. B, Vol 29B, No. 2, pp. 79-93.

[6] Daganzo, C. F. (1995b). Properties of Link Travel Time Functions under Dynamic Loads. Transpn. Res. B, Vol 29B, No. 2, pp. 95-98.

[7] Daganzo, C. F. (1995c). A finite difference approximation of the kinematic wave model of traffic flow. Transpn. Res. B, Vol 29, No. 4, pp. 261-276.

[8] Frank M. and P. Wolfe (1956). An algorithm for quadratic programming. Naval Research Logistics Quarterly, Vol 3, 95-110.

[9] Friesz, T., Bernstein, D., Smith, T., Tobin, R., and Wie, B.-W. (1993a). A variational inequality formulation of the dynamic network user-equilibrium problem. Operations Research, 41(1),179–191.

[10] Friesz, T., Luque, J., Tobin, R., and Wie B.-W. (1989). Dynamic network traffic assignment considered as a continuous time optimal control problem. Operations Research, 37(6):893–901.

[11] Gerlough, D. L. and Huber, M. J. (1975). Traffic Flow Theory: A Special Report. Special Report no. 165. Transportation Research Board, Washington, DC.

[12] Heidemann, D. (1999). Some critical remarks on a class of traffic flow models. Transporation Research B 33, No. 2, pp.153–155.

[13] Herman, R., Montroll, E. W., Potts, R. B. and Rothery, R. W. (1959). Opns. Res., Traffic dynamics: Analysis of stability in car following, Vol. 7, pages 86–106.

[14] Jayakrishnan, R., W. K. Tsai and A. Chen (1995). A Dynamic Traffic Assignment Model with Traffic-flow Relationships. Transpn. Res. Vol 3, No. 1, pp. 51-72.

[15] Kachani, S. and G. Perakis (2001a). Modeling Travel Times in Dynamic Transportation Networks; A Fluid Dynamics Approach. Working Paper, Operations Research Center, MIT.

[16] Kachani, S. and G. Perakis (2001b). Second-order Fluid Dynamics Models for Travel Times in Dynamic Transportation Networks. Proceedings of the 4th international IEEE conference on intelligent transportation systems, Oakland, California, 2001.

[17] Kachani, S. and G. Perakis (2001c). A Fluid Model of Spillback and Bottleneck Phenomena for Modeling Dynamic Travel Times. Working Paper, Operations Research Center, MIT.

[18] Kuwahara, M. and T. Akamatsu (2001). Dynamic user optimal assignment with physical queues for a many-to-many OD pattern. Transpn. Res. B, 35, pp. 461-479.

[19] LeVeque, R.J. (1990). Numerical Methods for Conservation Laws. Birkhäuser-Verlag.

[20] Lighthill, M. J. and J. B. Whitham (1955). On Kinematic Waves. I: Flow Movement in Long Rivers; II: A Theory of Traffic Flow on Long Crowded Roads. Proc. Royal Soc. A, 229, pp. 281-345.

[21] Magnanti, T. and Perakis, G. From Frank-Wolfe to steepest descent; a descent framework for solving asymmetric variational inequalities, Working Paper, ORC, MIT, 1998.

[22] Menguzzer, C., D. E. Boyce , N. RouphaiL and A. Sen (1990). Implementation and Evaluation of an Asymmetric Equilibrium Route Choice Model Incorporating Intersection-Related Travel Times. Report to Illinois Department of Transportation, Urban Transportation Center, University of Illinois, Chicago.

[23] Papageorgiou M. (1983). Applications of automatic control concepts to traffic flow modeling and control. Springer Verlag, Berlin.

[24] Papageorgiou M. (1998). Some remarks on macroscopic flow modeling. Transportation Research A, 32, (5):323–329.

[25] Papageorgiou M., Blosseville J. M. and Haj-Salem H. (1989). Macroscopic modeling of traffic flow on the boulevard peripherique in Paris. Transportation Research B, 23, 29–47.

[26] Payne, H. J. (1971). Models of freeway traffic and control. in G.A. Bekey, editor. Mathematical Models of Public Systems, volume 1 of Simulation Councils Proc. Ser., pages 51–60.

[27] Perakis, G. (2000). Dynamic Traffic Flow Network Problems; a Hydrodynamic Theory Approach. Working paper, Operations Research Center, MIT.

[28] Perakis, G. and M. Zaretsky (2002). On the Efficient Solution of Variational Inequalities: Complexity and Computational Efficiency. Working paper, Operations Research Center, MIT.

[29] Pipes, L. A. (1953). An operational analysis of traffic dynamics. J. Appl. Phys., (24),274–281.

[30] Ran, B. and D. E. Boyce (1994). Dynamic Urban Transportation Network Models: Theory and Implications for Intelligent Vehicle-Highway systems. Springer-Verlag.

[31] Ran, B., R. W. Hall and D. E. Boyce (1996). A Link-based Variational Inequality Model for Dynamic Departure Time/route Choice. Transpn. Res. B, Vol. 30, No.1, pp. 31-46.

[32] Reuschel, R. (1950). Fahrzeugbewegungen in der kolonne bei gleichformig beschleunigtem verzogertem leitfahrzeug. Z. Osterr. Ing. Arch. Ver., (95),52–62.

[33] Richards, P. I. (1956). Shockwaves on the Highway. Operations Research. 4, pp. 42-51.

[34] Transportation Research Board (TRB) (1997). Traffic Flow Theory.

[35] Wardrop, J. G. (1952). Some Theoretical Aspects of Road Traffic Research, Proceedings of the Institute of Civil Engineers, Part II, 1, 325-378.

[36] Whitham, G. B. (1974). Linear and Nonlinear Waves. John Wiley and Sons, New York, pp. 68-95.

[37] Xu, Y. W., J. H. Wu , M. Florian , P. Marcotte and D. L. Zhu (1999). Advances in the Continuous Dynamic Network Loading Problem. Transportation science, Vol 33, No. 4, pp. 341-353.

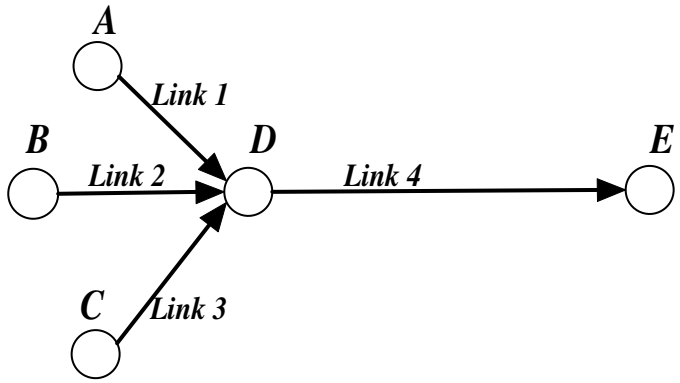

Figure 1: Network 1, a simple example network

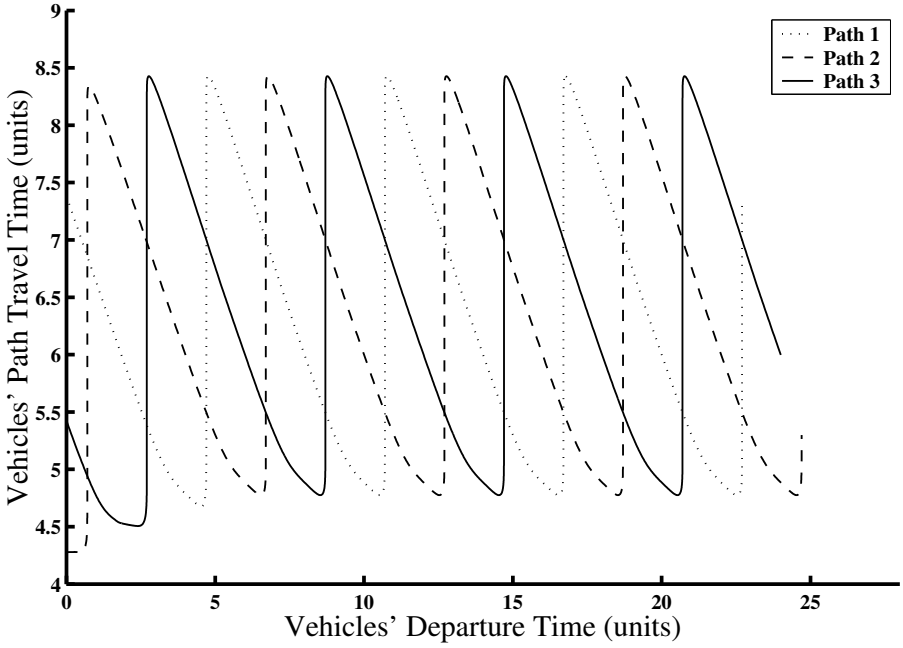

Figure 2: Path travel times by using hyperbolic PDE method, network 1

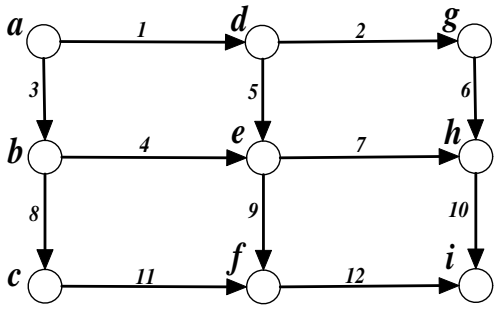

Figure 3: Network 2, a more complex example network

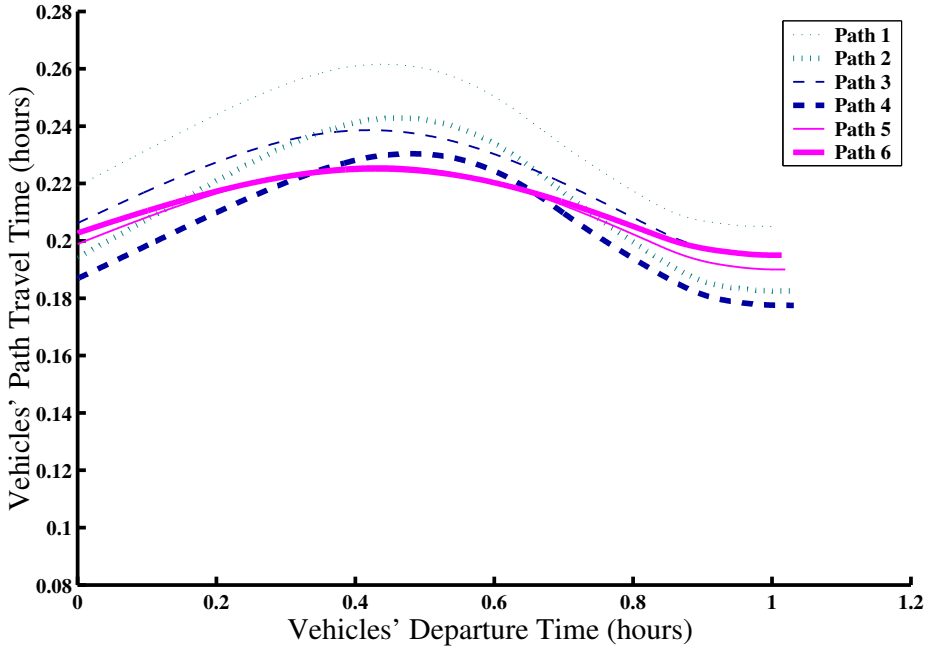

Figure 4: Path travel times by using hyperbolic PDE method, network 2 (Part I)

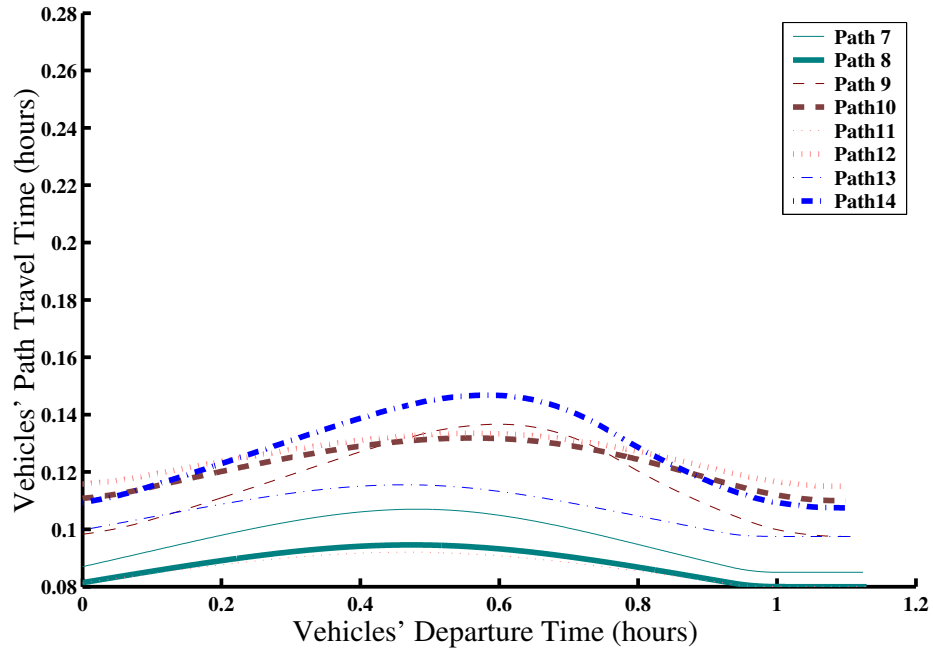

Figure 5: Path travel times by using hyperbolic PDE method, network 2 (Part II)

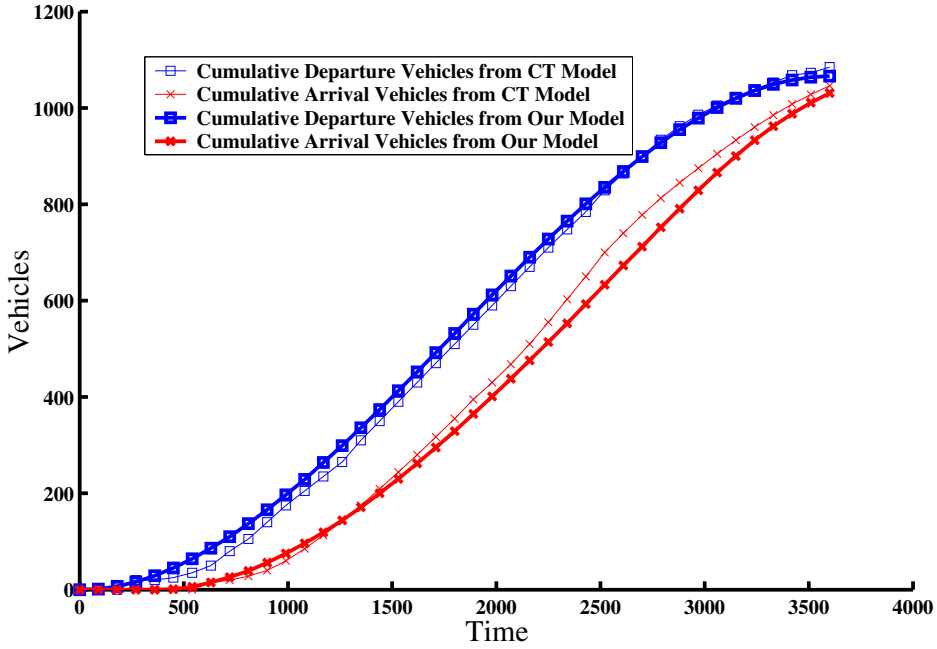

Figure 6: The cumulative departure/arrival vehicle number by our model and CT model

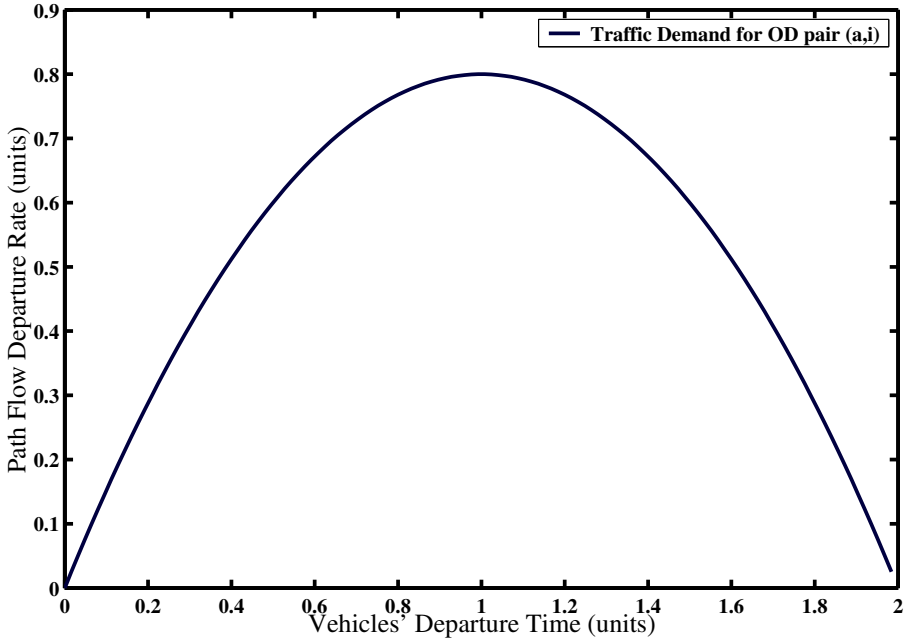

Figure 7: O-D pairs demand for O-D pair (a,i)

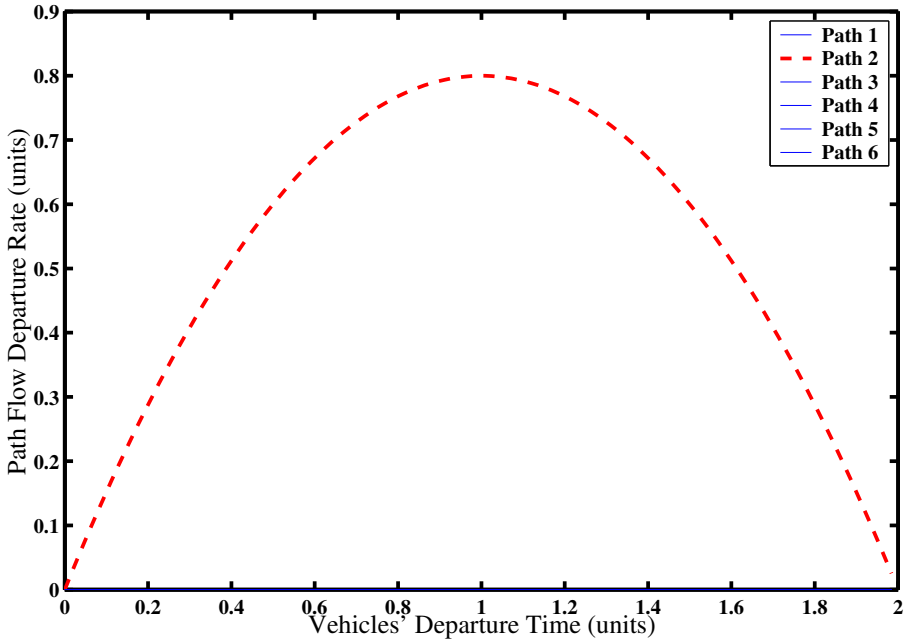

Figure 8: Initial traffic assignments for O-D pair (a,i)

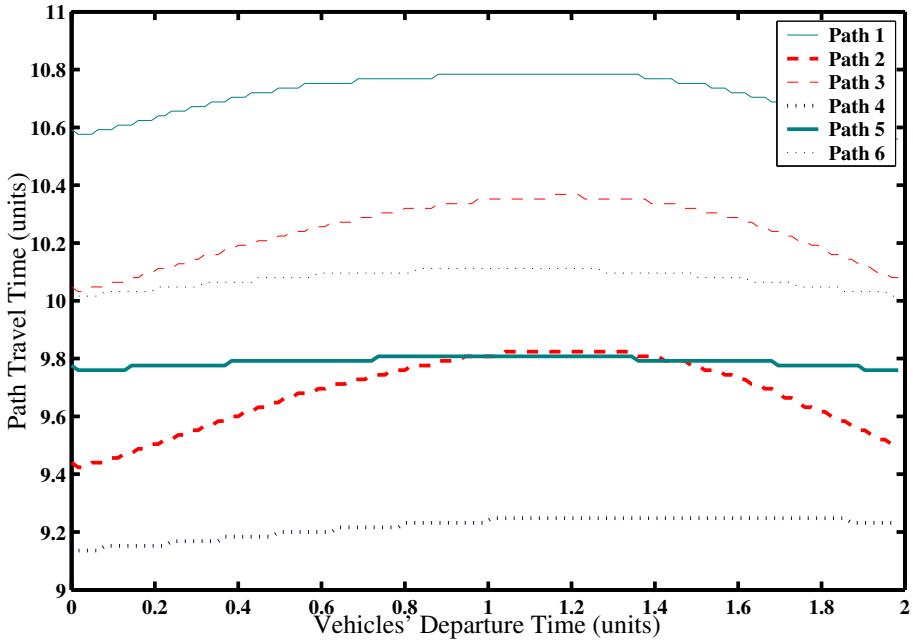

Figure 9: Initial Path Travel Times for O-D pair (a,i)

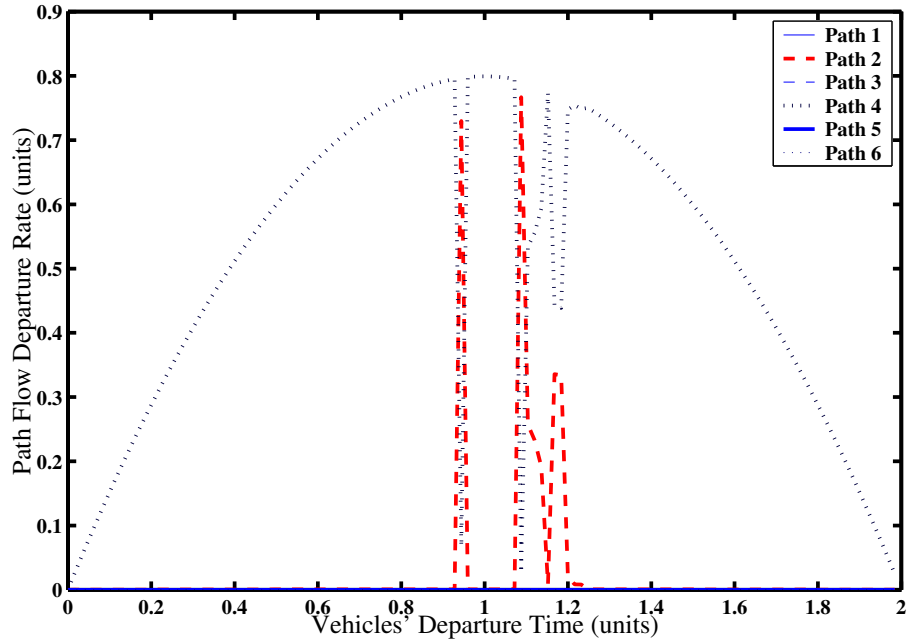

Figure 10: Equilibrium-satisfying traffic assignments for O-D pair(a,i)

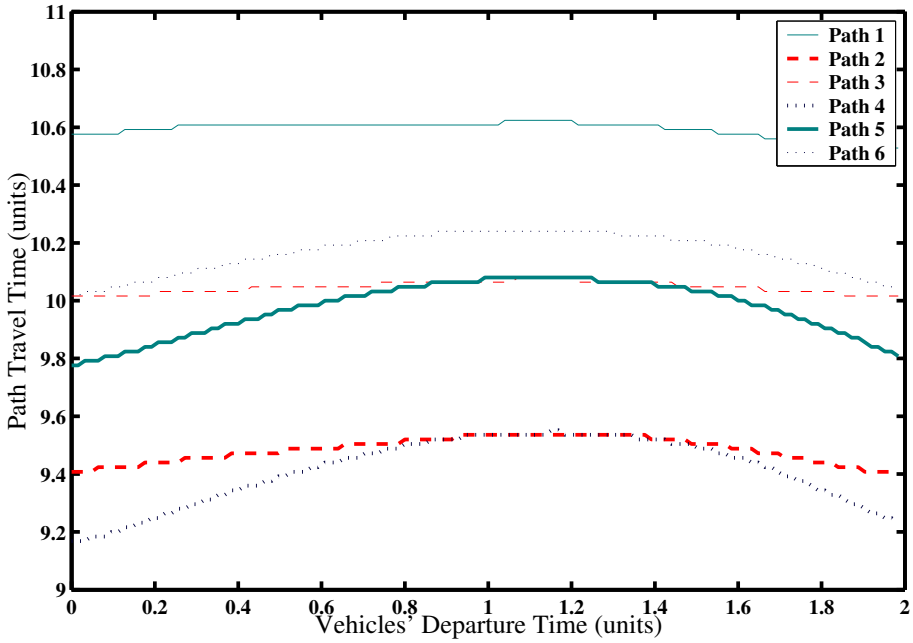

Figure 11: Equilibrium-satisfying path travel times for O-D pair(a,i)

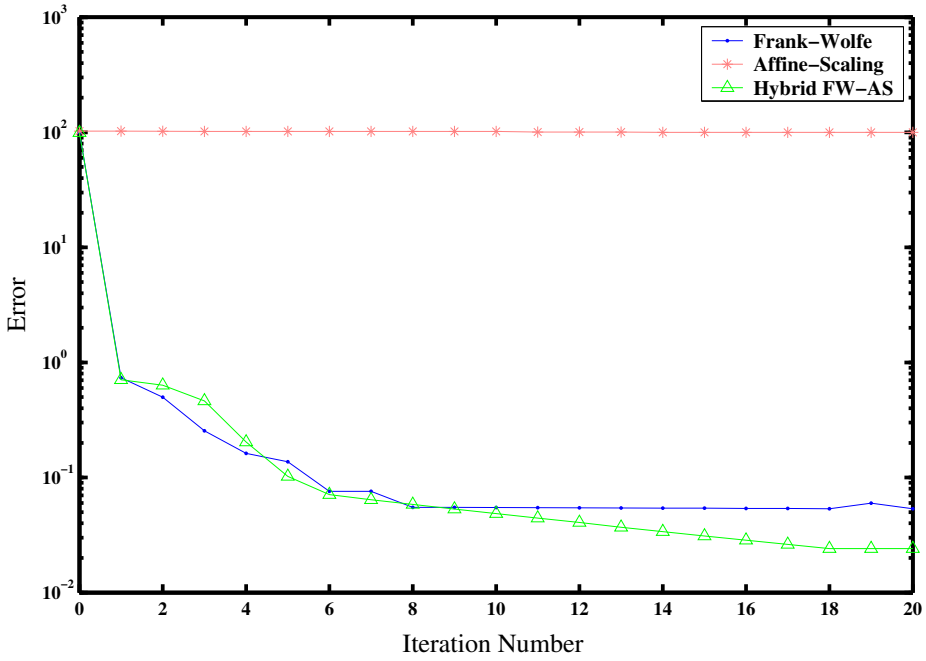

Figure 12: Convergence plot for three different solution methods

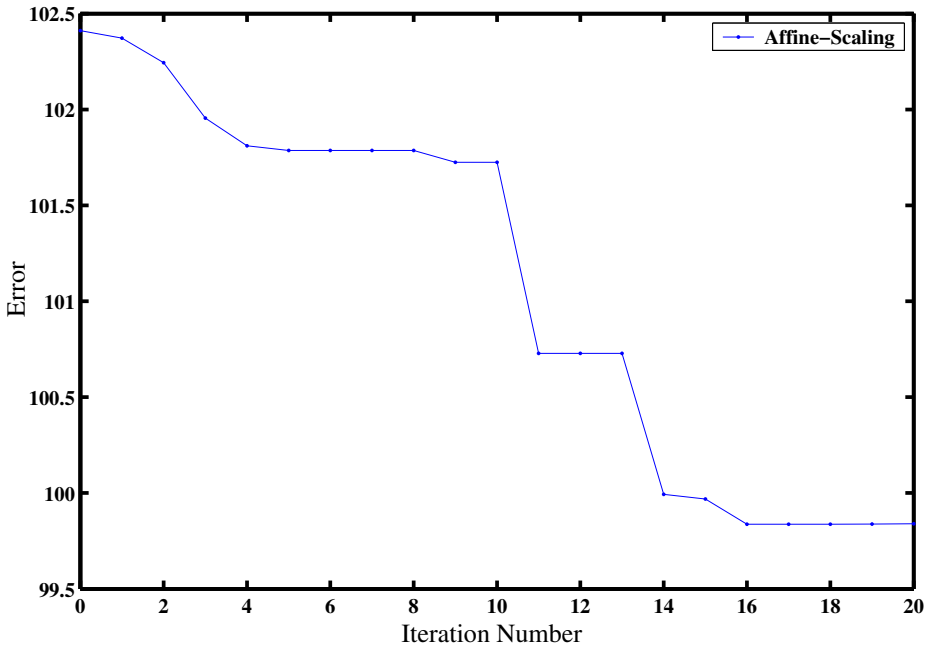

Figure 13: Convergence plot for Affine-Scaling version of FW method in a larger scale